

Numerical modeling of heat transfer process in transverse section of a plate heat exchanger

Cite as: AIP Conference Proceedings **2486**, 020022 (2022); <https://doi.org/10.1063/5.0105575>
Published Online: 15 November 2022

Y. V. Vankov, E. V. Izmaylova, E. V. Garnyshova, et al.



View Online



Export Citation

1.8 GHz

8.5 GHz

Trailblazers. New

Meet the Lock-in Amplifiers that measure microwaves.

Zurich Instruments [Find out more](#)

Numerical Modeling of Heat Transfer Process in Transverse Section of a Plate Heat Exchanger

Y. V. Vankov¹, E. V. Izmaylova^{1, a)}, E. V. Garnyshova¹, A. M. Khvorystkina¹
and I. V. Shvetsov^{2, b)}

¹ Kazan State Power Engineering University, Kazan, Russia

² Yaroslav-the-Wise Novgorod State University, Veliky Novgorod, Russia

^{a)} Corresponding author: evgeniya-izmailova@yandex.ru

^{b)} Igor.Shvetsov@novsu.ru

Abstract. Heat exchangers make up a large group of heat-power equipment, so the right choice of heat exchangers is an important task. In this paper, a numerical experiment was carried out with the created models of plate water heat exchangers with different plate shapes in the ANSYS Workbench software package. Boundary conditions were formulated for all four types of plate heat exchanger, which, as a result of calculating and processing the results obtained, revealed the values of temperature and pressure at the outlet of the heat exchanger channels. Based on these data, the local resistance coefficients ζ and the temperature efficiency E_t were calculated for each heat exchanger model, and the influence of the plate shape on the increase in temperature efficiency and on the increase in pressure losses was also determined.

INTRODUCTION

Currently, more and more attention is paid to the problem of energy saving in heat supply systems. Heat exchangers make up a large group of heat-power equipment, occupying significant production areas and often exceeding 50% of the cost of a complete set in the heat power engineering, chemical and oil refining industries and a number of other industries. Therefore, the correct choice of heat exchangers appears to be an important task [1].

Heat exchangers are devices in which heat is transferred from one working medium to another. Reliable and efficient performance of the heat exchanger is an integral part of solving the problem of energy saving in heat supply systems. Due to the insufficiently efficient operation of these devices irrational losses of heat frequently increase 20 % of the volume of heat transferred. Such losses occur due to the inefficiency of the current outdated heat exchange equipment in the systems [2].

Plate heat exchangers are an integral part of modern heat supply systems which, thanks to their advantages, can significantly increase the efficiency of the system [3]. However, these heat exchangers also have certain disadvantages, the elimination of which will increase both the thermal and operational efficiency of the apparatus as well as of the whole system. One of the possible ways to increase energy efficiency of the plate heat exchanger is to improve the shape of heat transfer plates of the apparatus. Today, this issue has not been completely studied, but, undoubtedly, it is relevant [4–5].

The research purpose is to increase energy efficiency of the plate water heat exchanger by means of changing shapes of heat transfer plates [6].

The task is to carry out a numerical experiment with created models of plate water heat exchangers with different plate shapes in the ANSYS Workbench software package, which includes:

- 1) construction of a two-dimensional sketch of the models under consideration in the AutoCAD system of computer-aided design and drawing;
- 2) 3D-modeling of the examined models in the ANSYS Discovery SpaceClaim with the creation of a calculation mesh in the Watertight Geometry Workflow subroutine in Ansys Fluent Meshing;
- 3) calculation of the models with preset boundary conditions, working media properties, calculation model and convergence criteria; obtaining results and analyzing the data obtained;
- 4) comparison of models, construction of dependencies, graphs, analysis of the feasibility of their application and selection of the most optimal type of heat transfer plates to use in the plate water heat exchanger.

DESCRIPTION OF EXAMINED SAMPLES AND CONSTRUCTION OF CALCULATION MODELS

The 3-dimensional problem was solved. Boundary conditions for all four types of the plate heat exchanger were formulated, as a result of calculating and processing the data obtained the values of temperature and pressure at the outlet of channels of the heat exchanger were revealed [7]. Based on these data, the ζ coefficients of local resistance and the E_t temperature efficiency for each heat exchanger model were calculated. Also, the influence of the plates shape on the increase in temperature efficiency and the growth of pressure losses was determined. The models under consideration are presented in Fig. 1–4 [8–10].

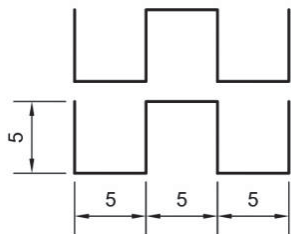


FIGURE 1. Calculation diagram of heat exchanger with channels of a square structure

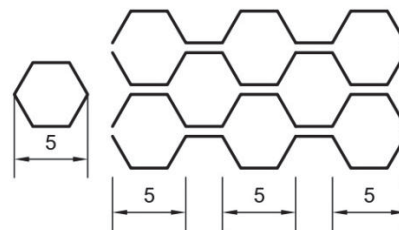


FIGURE 2. Calculation diagram of a heat exchanger with "honeycomb" channels

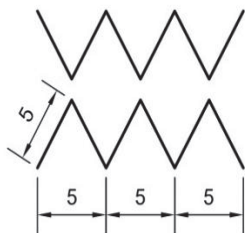


FIGURE 3. Calculation diagram of a heat exchanger with crankle plates

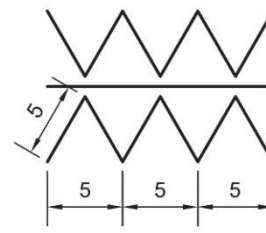


FIGURE 4. Calculation diagram of a heat exchanger with crankle and straight plates

Temperature efficiency is calculated according to the formula:

$$E_t = \frac{t_{\text{heated}} - t_{\text{cold}}}{t_{\text{warm}} - t_{\text{cold}}}, \quad (1)$$

where $t_{\text{heated}}, t_{\text{cold}}, t_{\text{warm}}$ – temperatures of heated, cold and warm water, °C.

The calculated total pressure losses in the channels are found, their values are averaged and the coefficient of local resistances of the apparatus is calculated according to the formula:

$$\zeta = \frac{\Delta P_n}{P_0}, \quad (2)$$

where ΔP_n is an averaged value of the total pressure drop, Pa;

P_δ is the value of dynamic pressure, Pa;

$$P_\delta = \frac{\rho \cdot v^2}{2} \quad (3)$$

ρ, v are density and speed at the entrance to channels, m/s.

CREATION OF CALCULATION MESH

The sizes of channels are taken such that their equivalent diameter lies in the range from 4 to 5 mm [11–12]. To average data, several such channels are made: half of the channels for cold water to flow, the other half for hot water to flow. Since a real heat exchanger cannot be designed due to limitation of calculating powers, the number of channels with hot and cold water is taken so that, as a result, we can have several channels with cold water completely surrounded by warm water. It is through these channels that the weighted average values of modeling results will be drawn out.

After correlating the elements into the desired groups, the plane is created, which is extended to create a three-dimensional model. The channel length is assumed to be 100 mm. Calculation models for each of the four types of plates are presented in Fig. 5–8 [13–14].

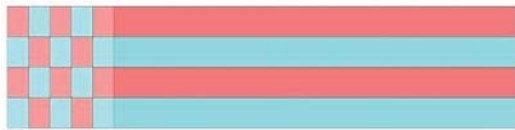


FIGURE 5. Calculation model of heat transfer plates with channels of a square structure

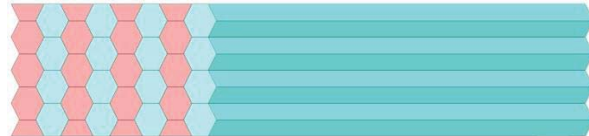


FIGURE 6. Calculation model of heat exchange plates with "honeycomb" channels

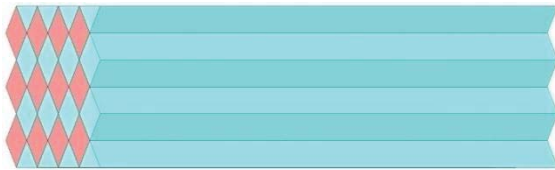


FIGURE 7. Calculation model of heat transfer plates with crangle plates

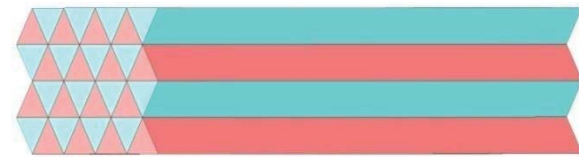


FIGURE 8. Calculation model of heat transfer plates with crangle and straight plates

The process of creating three-dimensional elements in the Watertight Geometry Workflow in the Ansys Fluent Meshing is similar to that described for modeling the heat exchange process in a longitudinal section. The modeling results are presented in Fig. 9–12. The different surface colors show the boundaries of the channel surfaces.



FIGURE 9. Three-dimensional model of heat transfer plates of a square structure



FIGURE 10. Three-dimensional model of heat exchange plates with "honeycomb" channels



FIGURE 11. Three-dimensional model of plates with crinkle plates



FIGURE 12. Three-dimensional model of heat transfer plates with crinkle and straight plates

The data about the meshes of the models are shown in tables 1–4.

TABLE 1. Data of the obtained meshes of heat transfer plates with channels of a square structure

	Boundary	Internal
Nodes	571 969	4 5227 894
Faces	209 961	6 980 281
Total number of calculation meshes		1 348 577

TABLE 2. Data of the obtained meshes of heat exchange plates with channels of “honeycomb” structure

	Boundary	Internal
Nodes	819 815	5 446 566
Faces	319 239	8 134 538
Total number of calculation meshes		1 498 420

TABLE 3. Data of the obtained meshes of heat transfer plates with crinkle plates

	Boundary	Internal
Nodes	723 749	5 045 859
Faces	270 236	7 883 320
Total number of calculation meshes		1 534 346

TABLE 4. Data of the obtained meshes of heat transfer plates with crinkle and straight plates

	Boundary	Internal
Nodes	642 314	3 828 593
Faces	242 465	6 215 051
Total number of calculation meshes		1 252 785

At the following stage the conditions of convergence of all parameters are set. Then the number of iterations is set, which are necessary in case the program will not reach the convergence, and the calculation will stop at the preset number of iterations.

To analyze the models, it is necessary to create a two-dimensional plane, on which necessary calculation results will be graphically displayed: the values of temperature, velocity, turbulence, pressure. To create a plane, the coordinate of the initial point is set, as well as the normal along which the plane will be drawn (Fig. 13–16). The plane for the results to be displayed is formed by the normal and point, from which it will be drawn.

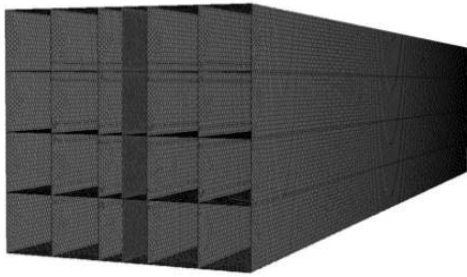


FIGURE 13. Plane for displaying the graphical calculation results of the model with channels of a square structure

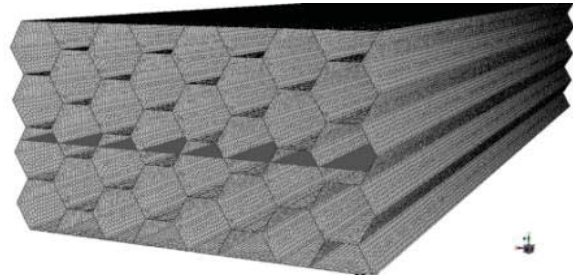


FIGURE 14. Plane for displaying the graphical calculation results of the model with the channels of a “honeycomb” structure

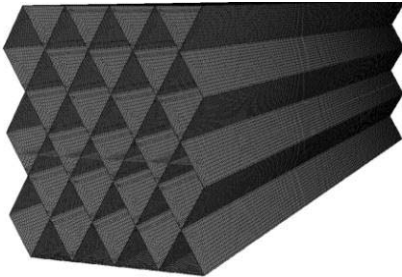


FIGURE 15. Plane for displaying the graphical calculation results of the model with crinkle plates

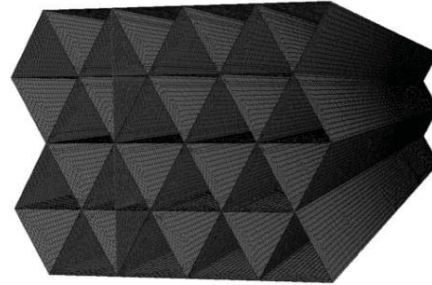


FIGURE 16. Plane for displaying the graphical calculation results of the model with crinkle and straight plates

CALCULATION AND ANALYSIS OF THE DATA OBTAINED

The flow of fluid is considered at speeds of 0.01 m/s, 0.05 m/s, 0.1 m/s, 0.2 m/s. Longitudinal and transverse profiles of flow temperatures at speeds of 0.01 m/s and 0.1 m/s for the models with the channels of a square structure are shown in Fig. 17–19.

Images present the profiles of temperature and scale which serve to correlate a flow color with a specific temperature value. The longitudinal and transverse sections show that the flows are similarly heated but at the exit from the channel the low sites significantly differ from the rest of the flow. This is associated with the fact that at a speed of 0,01 m/s, at the exit from the channel, a reverse flow shown in Fig. 17 is formed, which additionally heats the flow.

Illustration of the channel fragment serves to evaluate the influence of the reverse flow on the final results of heating cold water. Due to the color scheme, you can notice that, before its appearance, the peripheral layers have already warmed up to the reverse flow temperature, while the central layers have had less time to be heated.

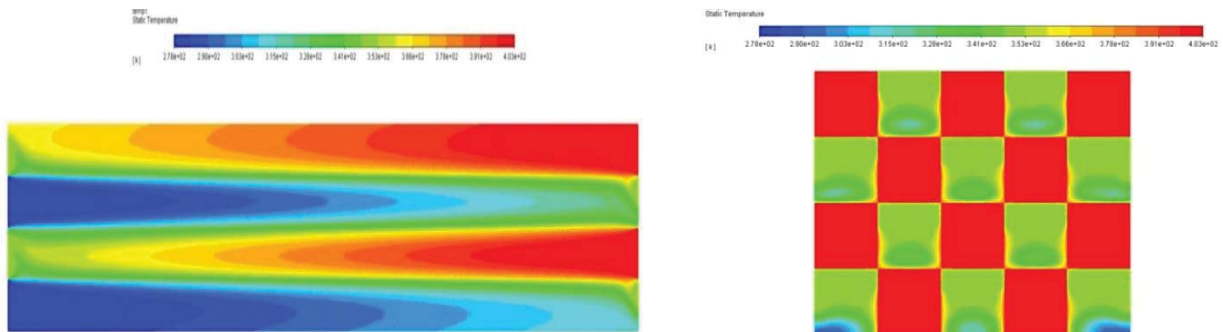


FIGURE 17. Longitudinal and transverse temperature profiles for the model with channels of a square structure at $v = 0.01 \text{ m/s}$

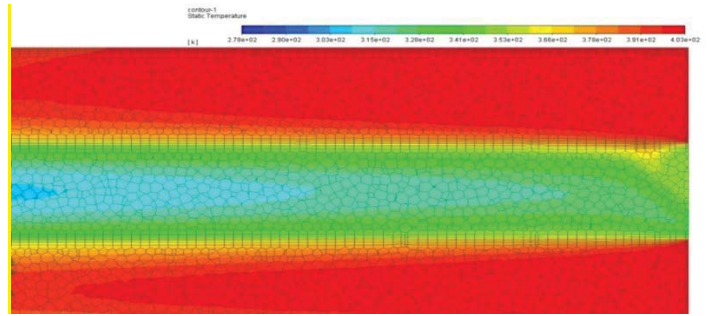


FIGURE 18. Fragment of the channel with a reverse flow

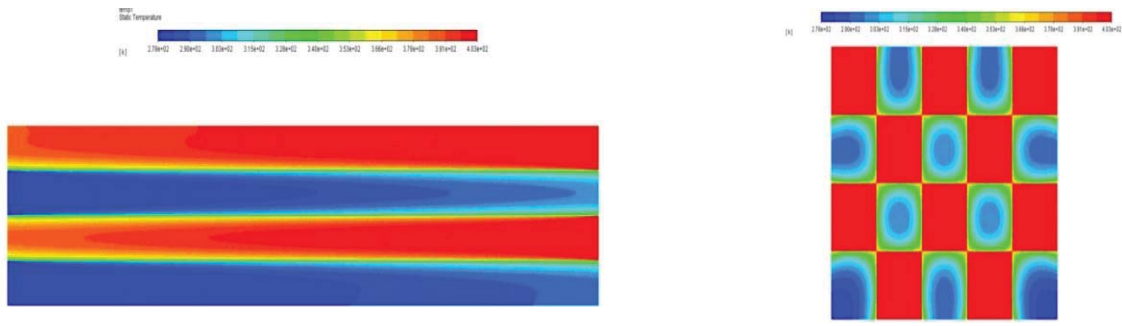


FIGURE 19. Longitudinal and transverse temperature profiles for the model with channels of a square structure at $v = 0.1 \text{ m/s}$

At a speed of 0,1 m/s the temperature efficiency dropped significantly, which is associated with the fact that, due to such shapes of the channels, the central fluid layer is distant from the walls of the heat exchanger. A reverse flow is absent.

Judging by the results, we can conclude that, with such configuration of the channels, the main flow heating occurs in the corners of the channel while in the middle of the channel it occurs to a much less extent. Also, on the longitudinal temperature profile, at a speed of 0.01 m/s, it is evident that at the exit from the channel there occurs a reverse flow which additionally “heats up” the flow. Judging by it, the outlet temperature should be taken lower than the average weighted value given by the program. The positive feature of this model is the low pressure loss.

The longitudinal and transverse profiles of the flow temperatures at speeds of 0.01 m/s and 0.1 m/s for the model with the channels of “honeycomb” structure are shown in Fig. 20–22.

By the calculation results it is evident that the flows are better heated that in the previous model, this is especially marked with a color range at the exits in the longitudinal section. At this speed, a reverse flow is observed just as in the channels of a square structure (Fig. 21).

As with the previous model, we can assess the effect of a reverse flow based on this fragment. In contrast to the previous model, the temperature of the reverse flow practically does not affect the obtained results, since we can observe in the image that, before the appearance of the reverse flow, the peripheral layers as well as central ones have almost warmed up to the temperature of the reverse flow.

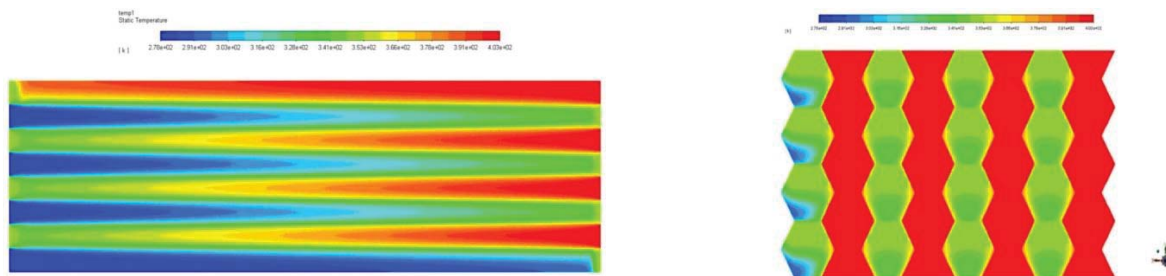


FIGURE 20. Longitudinal and transverse temperature profiles for the model with “honeycomb” channels at $v = 0.01 \text{ m/s}$

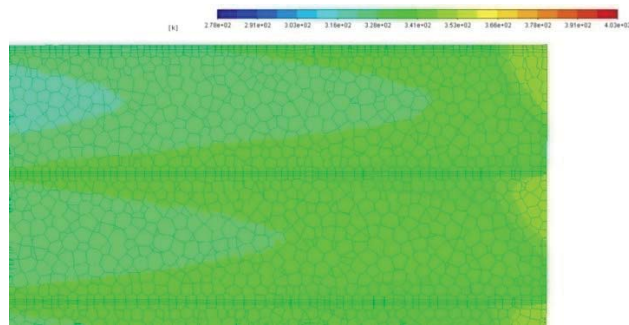


FIGURE 21. Fragment of the channel with a reverse flow

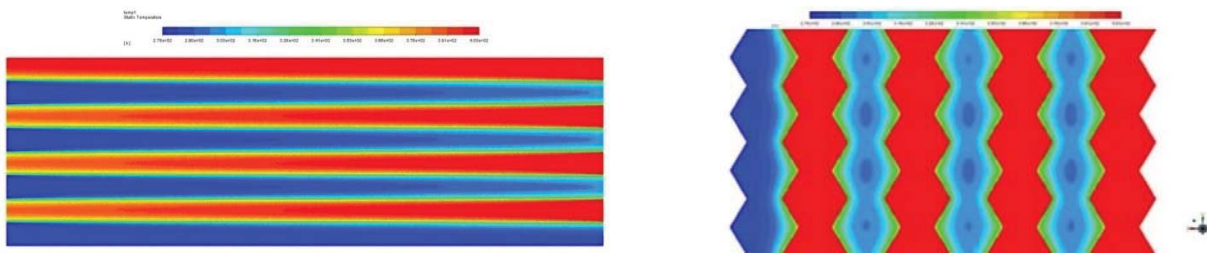


FIGURE 22. Longitudinal and transverse temperature profiles for the model with “honeycomb” channels at $v = 0.1 \text{ m/s}$

At a speed of 0.1 m/s the temperature efficiency drops sharply. The central layers of the flow are better involved in heat exchange, since they are closer to the adjacent walls. At the same time, the useful area of heat exchange is less, because flows with the same coolant are not staggered, as was the case with the previous model, but one above the other, due to which one third of the channel area does not participate in heat exchange which leads to the efficiency drop.

Based on the results, we can conclude that, with this configuration of the channels, the flow is heated not only along the perimeter, but also closer to its centre. Also, on the longitudinal temperature profile, at the end of the site, at a speed of 0.01 m/s the reverse flow is observed, but, unlike the channels with a square structure, the temperature of the reverse flow does not affect the obtained results. At lower speeds, such shape of a channel is more effective than a square one. There is no reverse flow.

The longitudinal and transverse profiles of flow temperatures at speeds of 0.01 m/s and 0.1 m/s for the model with crinkle plates are shown in Fig. 23–25.

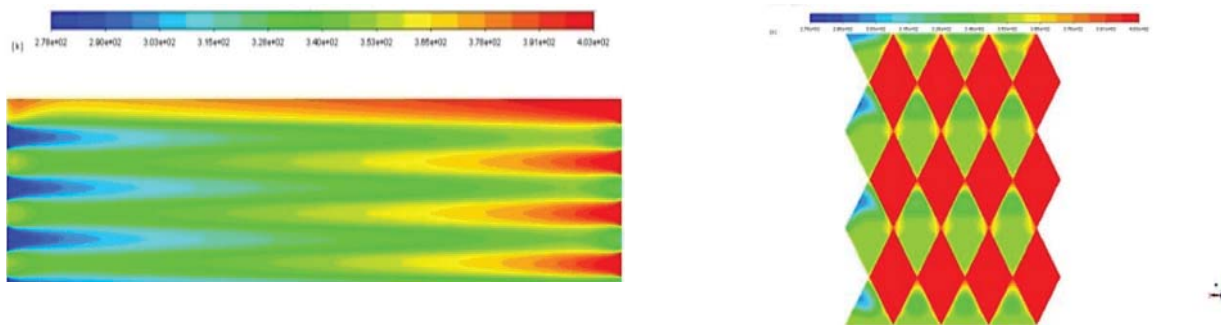


FIGURE 23. Longitudinal and transverse temperature profiles for the model with crinkle plates at $v=0.01 \text{ m/s}$

The images and colors of the flow demonstrate that, at low speeds, the flows of cold water are heated up better than in the previous models. In this model, at a speed of 0.01 m/s , the reverse flow is also formed (Fig. 24).

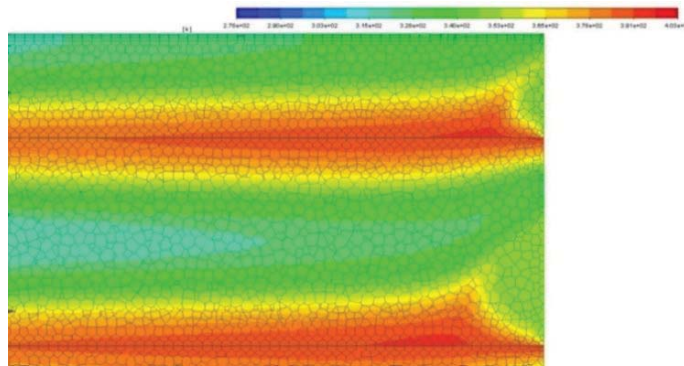


FIGURE 24. Fragment of the channel with a reverse flow

In the presented image we can notice that, before the appearance of the reverse flow, the layers at the periphery have already been heated up above the temperature of the reverse flow, and the central layers have been heated up to the temperature of the reverse flow.

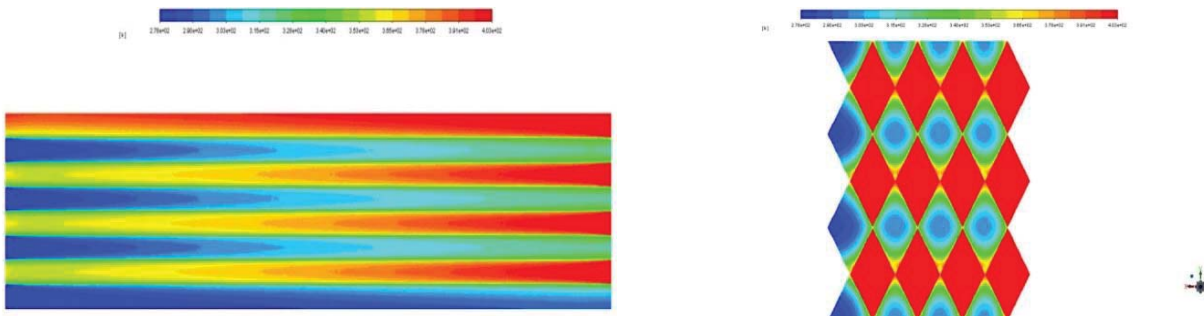


FIGURE 25. Longitudinal and transverse temperature profile for the model with crinkle plates at $v=0.1$ m/s

At a speed of 0,1 m/s the temperature efficiency dropped, but to a much lesser extent, than in the previous model. The central layers of the flow are better involved in the heat exchange than in the square channels, but in less than in the channels of “honeycomb” structure, but, due to the fact that the useful area is large, the final efficiency is higher. There is no reverse flow.

Based on the results, we can conclude that, with this configuration of the channels, the flow is heated practically over the entire area of the section. Also, on the longitudinal temperature profile, at a speed of 0.01 m/s, it is evident that at the exit from the channel there occurs the reverse flow just as in the square channels, however, in this case, the flow, on the contrary, is “cooled” by the reverse current. Judging by this, the outlet temperature should be taken higher than the average weighted value given by the program.

The longitudinal and transverse temperature profiles of the flows at speeds of 0.01 m/s and 0.1 m/s for the model with crinkle and straight plates are shown in Fig. 26, 27.

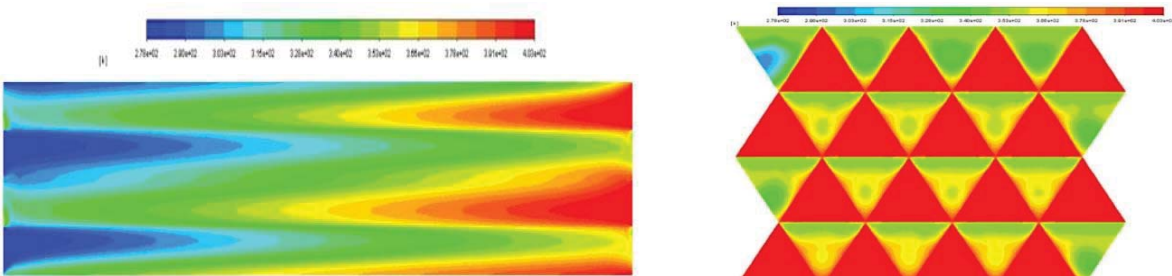


FIGURE 26. Longitudinal and transverse temperature profiles for the model with crinkle and straight plates at $v = 0.01$ m / s

These images and colors of the flow show that, at low speeds, the flows of cold water are heated up better than in the previous models. There is no reverse flow.

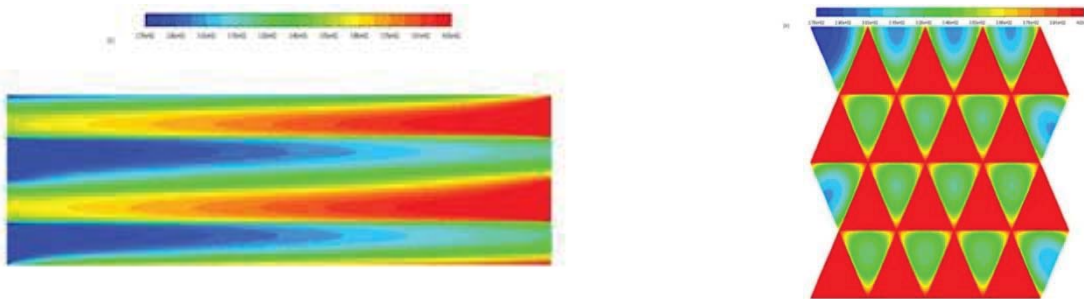


FIGURE 27. Longitudinal and transverse temperature profiles for the model with crackle and straight plates at $v=0.1$ m/s

In this case we can evaluate how the central layer is heated up. The distance from the center to periphery is minimum. The useful area is maximum in comparison to the other models, however, this increase in the contact area leads to increased pressure losses.

Based on the results, we can conclude that, with this configuration of the channels, the flow is heated more in the low part of the section. Also, on the longitudinal temperature profile, at a speed of 0.01 m/s, it is obvious that at the outlet of the channel there is no reverse flow. This is the most heat-efficient shape, however, its hydraulic losses are 2 and more times higher than those of the others.

The results of all the calculations made are presented in table 5.

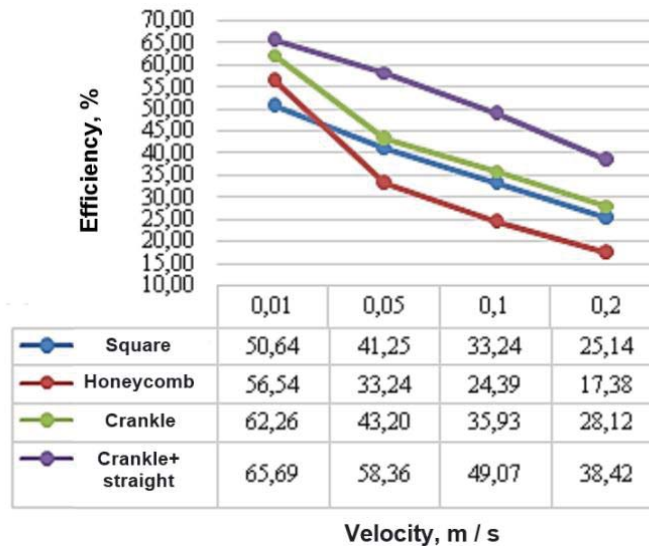


FIGURE 28. Efficiency versus flow rate graph

TABLE 5. Results of calculations made

Square structure	v, m/s	0.01	0.05	0.1	0.2
	T _{out} , K	341.30	329.57	319.55	309.42
	efficiency	50.64	41.25	33.24	25.14
	P before, Pa	2.45	14.98	39.71	112.64
	P after, Pa	0.32	1.73	6.31	24.28
	dP, Pa	2.13	13.26	33.40	88.35
	P _{dyn} , Pa	0.05	1.25	5.00	20.00
	KMC	42.65	10.61	6.68	4.42
Channels with “honeycomb” structure	T _{out} , K	348.67	319.55	308.49	299.73
	efficiency	56.54	33.24	24.39	17.38
	P before, Pa	3.13	19.51	48.82	128.00
	P after, Pa	0.27	1.64	6.14	23.84
	dP, Pa	2.86	17.87	42.68	104.16
	P _{dyn} , Pa	0.05	1.25	5.00	20.00
	KMC	57.29	14.30	8.54	5.21
Channels with crinkle plates	T _{out} , K	355.83	332.00	322.91	313.16
	efficiency	62.26	43.20	35.93	28.12
	P before, Pa	3.11	18.66	48.94	131.60
	P after, Pa	0.35	1.81	6.42	24.63
	dP, Pa	2.76	16.86	42.52	106.97
	P _{dyn} , Pa	0.05	1.25	5.00	20.00
	KMC	55.20	13.49	8.51	5.35
Channels with crinkle and smooth plates	T _{out} , K	360.11	350.95	339.33	326.02
	efficiency	65.69	58.36	49.07	38.42
	P before, Pa	5.59	35.70	88.28	229.38
	P after, Pa	0.20	1.71	6.44	24.75
	dP, Pa	5.39	34.00	81.84	204.63
	P _{dyn} , Pa	0.05	1.25	5.00	20.00
	KMC	107.75	27.20	16.37	10.23

Based on the data obtained, graphs of efficiency versus flow rate (Fig. 28) and total pressure losses versus flow rate (Fig. 29) were built.

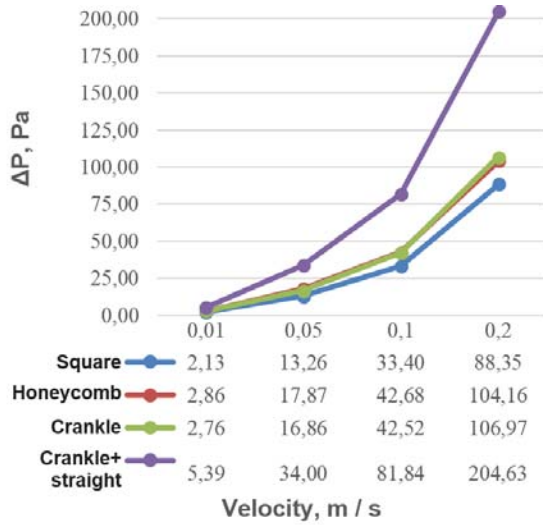


FIGURE 29. Total pressure loss versus flow rate graph

This graph demonstrates how the efficiency varies with the flow rate. A special attention should be paid to the fact that in general the tendency between the models is constant, except for the case when honeycombs are more efficient at low speeds. From this observation we can suppose that at relatively low speeds the distance from the centre of the flow to the periphery is more influential than the useful area, but with increasing speed the area becomes more important. This graph demonstrates that the latest model has the highest thermal efficiency.

From this graph we can conclude that, at low speeds, losses do not differ much, however, with increasing speed the difference becomes more evident. Although the latest model shows the highest efficiency, this occurs under the condition that, on average, pressure losses are 2 times higher than those of the other models. Based on the above, at relatively low speeds the best option will be the use of the latest model, but, with increasing speed, an optimal option is the model with crackle plates.

CONCLUSION

We performed a numerical modeling of heat transfer process in a plate heat exchanger in a transverse section with the help of the ANSYS software package. We considered four kinds of plates: with channels of a square structure, with channels of a “honeycomb” shape, with crackle plates, with crackle and straight plates.

Based on the research results, we can conclude that an important factor is the useful area of plates, which should be maximized. The concept of useful area means those adjacent walls, which contact with both cold and hot water. So, in the model with honeycomb-shaped channels, a honeycomb has 6 sides, with 2 of them in contact with cold environment. The lack of heat exchange degrades the efficiency of such plates, while in the channels with a square structure the contact area between environments is maximized, and, correspondingly, the thermal efficiency is higher. However, in the channels of a square structure the distance from the centre of the flow to the walls is greater, which, in contrast, has a negative effect at low speeds, if compared to the honeycombs.

Based on the data obtained, it can also be concluded that the distance to the centre of the flow should be minimized. In this case heating occurs throughout the entire volume of the coolant just as in the model with crackle plates.

Also, it should be noted that, due to different viscosities of media (in cold water the viscosity is higher than in hot water), the use of channels of different shapes will be. It is also worth noting that due to the different viscosities of the media (cold water has a higher viscosity than hot water), the use of different channel shapes will be most justified. To achieve the lowest hydraulic losses in cold water channels, it is necessary to use a more streamlined channel shape, which would minimize losses. At the same time, for hot flow channels the best solution would be to use channels that create more resistance, but give more heat transfer.

REFERENCES

1. B. S. Petukhova and V. K. Shikova, *Handbook of heat exchangers: Part 1* (translation from English) (Energoatomizdat, Moscow, 1987).
2. Zh. Ayub, Heat exchange equipment **24(5)**, 3-16, (2003).
3. Ju Lee Hyung and Lee Hyuk Seong, *Energies* **13(6)**, 1328 (2020).
4. A. Sadeghianjahromi, S. Kheradmand, H. Nematy, J. S. Liaw and C. C. Wang, *Energies* **11 (8)**, 1-9, (2018).
5. S. H. Lee, M. Lee, W. J. Yoon, and Y. Kim, *Int. J. Heat Mass Transfer* **34(1)**, 328-336 (2016). doi: 10.1016/j.ijrefrig.2010.08.013
6. E. Martinez, W. Vicente and M. Salinas-Vazquez, *Appl. Therm. Eng.* **110**, 306-317 (2017).
7. H. E. Gallus, *Recent Research Work on Turbomachineiy Flow* (Yokohama International Gas Turbine Congress, Yokohama, 1995).
8. F. R. Menter, *AIAA-Journal*. **32 (8)**, 1598-1605 (1994).
9. H. Schlichting, *Experimentelle Untersuchungen zum Rauigkeitsproblem* (Ing.-Arch. 7: NACA Tech. Mere., 2006).
10. M. Picon-Nunez, G. T. Polley and D. Jantes-Jaramillo, *Heat Transfer Engineering*. **31 (9)**, 742-749 (2010).
11. S. Perry, J. Klemes and I. Bulatov, *Energy*, **33 (10)**, 1489-1497 (2008).
12. L. Wang, B. Sunden, R. M. Manglik, *PHE Design, applications and performance* (WIT Press; Southhampton, UK, 2007).
13. Q. W. Wang, M. Lin and M. Zeng, *App. Therm. Eng.* **29 (14-15)**, 3006-3013 (2009).
14. T. S. Khan, M. S. Khan, M-C. Chyu and Z. H. Ayub, *App. Therm. Eng.* **30 (8-9)**, 1058-1065 (2010).